A Density Functional Study of the ^{13}C NMR Chemical Shifts in Fluorinated Single-Walled Carbon Nanotubes†

Eva Zurek,‡,§ Chris J. Pickard,|| and Jochen Autschbach*,⊥

Max-Planck-Institut für Festkörperforschung, Heisenbergstrasse 1, 70569, Stuttgart, Germany, School of Physics & Astronomy, University of St. Andrews, St. Andrews KY16 9SS, Scotland, and Department of Chemistry, State University of New York at Buffalo, Buffalo, New York 14260-3000

Received: November 30, 2008; Revised Manuscript Received: January 9, 2009

The ^{13}C NMR chemical shifts of fluorinated semiconducting single-walled carbon nanotubes (SWNTs) were computed using a gauge−including projector−augmented plane wave (GIPAW) density functional method. The chemical shifts of the fluorinated carbons (C_α) were rather insensitive to the degree and pattern of functionalization, as well as to the nanotube radius. The calculated shifts were typically between 82 and 84 ppm, which is in excellent agreement with a recent experimental value of 83.5 ppm. Because of the insensitivity of the shifts to details of the nanotube's electronic structure and diameter, the NMR signals of the C_α carbons are a useful indicator of the degree of functionalization in a heterogeneous bulk sample. At high degrees of functionalization, the shifts of atoms neighboring C_α might also be useful indicators of the functionalization pattern.

I. Introduction

A substantial amount of research has been directed toward single-walled carbon nanotubes (SWNTs) due to their potential applications in many diverse areas. To cite but a few examples, it has recently been proposed that SWNTs may be employed as interconect wires in integrated circuits,[1] in optoelectronic devices,[2] or in sensing applications.[3,4] Moreover, chemical functionalization of the tubes can make them soluble in aqueous media and therefore potentially useful in biomedical applications.[5,6]

SWNTs may be functionalized with fluorine up to a saturation stoichiometry of C_2F without destroying the tubes.[7] The fluoronanotubes (F-SWNTs) can be used as versatile precursors for the preparation of covalently functionalized SWNTs via further derivatization.[5,8] For example, the fluorines may be replaced with alkyl groups,[9] as well as urea, guanidine, and thiourea.[10] Diamines[11] and diols[12] react with the F-SWNTs via nucleophilic substitution. It is also possible to covalently attach polymers to the nanotube sidewall.[13] The F-SWNTs can be dealkylated via dispersion in organic solvents, followed by heating.[5] Long F-SWNTs may be cut into shorter ones by thermolysis.[14,15]

A variety of methods including STM,[16] TEM,[7] as well as IR,[15] X-ray photoelectron spectroscopy,[10] and Raman[10] have been employed to characterize F-SWNTs. Recently it has been argued that Raman spectroscopy should be used cautiously for quantifying the extent of SWNT functionalization.[17]

Among the most frequently used tools to study the *local* geometry and electronic structure of molecules and solids is nuclear magnetic resonance (NMR). Over the past few years, an increasing amount of experimental and theoretical NMR data for SWNTs is becoming available; see refs 18−25 and references cited within. In particular, NMR has been used to characterize functionalized SWNTs. For example, in order to determine if the functional groups are covalently bound (rather than simply absorbed) to the surface of the SWNTs ^{13}C NMR experiments have been carried out.[26,27] In another study NMR provided evidence of the spatial proximity of the nanotubes and the functional group.[28] These works have demonstrated that direct observation of the signals of functionalized sidewall carbons (formally sp^3 hybridized) is observable in NMR experiments of nanotubes.

On the theoretical side, our first-principles theory based computations showed that the NMR of functionalized SWNTs is potentially very rich in information.[19−21] For covalent functionalizations, our calculations indicated that NMR may potentially be used to determine which bond is functionalized and the diameter distribution within the sample.[21,20] We have also shown that the NMR signals of SWNTs are quite sensitive to the presence of Stone−Wales defects.[24] Other authors have recently investigated the magnetic shieldings calculated inside the centers of the SWNTs, as well as in the center of their sidewall rings,[29−32] potentially indicating aromaticity stabilization of the sidewall and interesting NMR effects on molecules encapsulated in nanotubes.

A recent study on F-SWNTs proposed that, for high degrees of functionalization, NMR provides a better quantification of the degree of functionalization than Raman spectroscopy.[27] The ^{13}C NMR shift for the fluorinated sp^3 carbons in the nanotube sidewall was observed at $\delta = 83.5$ ppm. Calculations on a finite model for a fluorinated (5,5) SWNT based on a hydrogen end-capped $C_{80}H_{20}$ fragment led to the conclusion that this shift is indicative of 1,2-addition, rather than 1,4-addition of fluorine. However, only a single finite fragment was considered. Previous work has demonstrated that the addition energy of fluorine to a finite (5,5) tube depends strongly on the length of the fragment used.[33] Could the NMR chemical shifts for F-SWNTs also depend upon the length of the fragment? Is there a diameter dependence? We have previously shown that the ^{13}C chemical shifts of pristine and covalently (C−NR) functionalized SWNTs are dependent upon their capping mode, diameter, and length.[22,23]

† Part of the "George C. Schatz Festschrift".

* Address correspondence to this author. E-mail: jochena@buffalo.edu.
‡ E-mail: e.zurek@fkf.mpg.de or ez56@cornell.edu.
§ Max-Planck-Institut für Festkörperforschung.
|| University of St. Andrews.
⊥ State University of New York at Buffalo.

10.1021/jp810523x CCC: $40.75
Published on Web 02/24/2009

Therefore, it is important to investigate if the results of ref 27 obtained for a finite SWNT fragment can be extended to infinite F-SWNTS and varying diameters.

Herein, we employ first-principles theory to calculate the ^{13}C NMR chemical shifts of infinite F-SWNTs with finite band gaps. Different modes of addition of fluorine (i.e., 1,2 vs. 1,4) as well as various fluorinated isomers are considered. In previous work, we observed some dependence of the NMR signal on the pattern and degree of functionalization. To make a logical connection with these previous studies, we have decided to first look at F-SWNTs with a low to medium degree of functionalizion, and then compare the results to those obtained for tubes with C_2F stoichiometry (saturation). The effects from varying diameters of the F-SWNT on the shifts of the sp^3 carbons are also examined, along with a number of different substitution patterns. Geometrical parameters, band gaps, and binding energies of the F-SWNTs are provided.

Our calculations show that the position of the chemical shift of carbons bound to fluorine is very robust and in general it is not sensitive to the diameter nor the degree or pattern of functionalization. We obtain shifts that are very similar to the 83.5 ppm reported in ref 27. Therefore, this ^{13}C signal is indeed a very good experimental indicator of the degree of SWNT fluorination. On the other hand, our calculations indicate that the band structures depend strongly on the degree and pattern of functionalization.

In Section II computational details are provided. Results are reported in Section III, first focusing on structures, fluorination energies, and band gaps (Section 3A). In Section 3B, we consider the NMR parameters of a selection of fluorinated zigzag SWNTs. Some conclusions are provided in Section IV.

II. Methodology: Computational Details

The computations employed a plane-wave based density functional theory (DFT) first-principles method as implemented in a developer's version of the Castep code.[34,35] We have used the Perdew−Burke−Ernzerhof (PBE)[36] density functional along with ultrasoft pseudopotentials.[37] The plane-wave basis energy cutoff was 420 eV for the pristine tubes, and 555 eV for the F-SWNTs and the F_2 molecule. Isolated infinite SWNTs were calculated by using a hexagonal unit cell of appropriate size in the a, b direction to ensure an inter-tube separation of at least 8 Å, as described previously.[22] All structures were fully optimized.

NMR shielding tensors were calculated by using a gauge-including projector-augmented plane-wave (GIPAW) approach extended to ultrasoft pseudopotentials.[38,39] The computational settings were carefully benchmarked in ref 22 and are described extensively in refs 21 and 22. The reciprocal space grids ("k-grids") necessary to obtain converged chemical shifts are provided in Table 1. Here, we also provide the size of the supercells used, C:F ratio, and list the types of $(n, 0)$ tubes studied. Band gaps, binding energies, and geometrical parameters converge with fewer k-points. If the shielding constants obtained from a (1,1,m) and a (1,1,m+1) k-grid differed by more than 0.5 ppm for any of the atoms in the unit cell, an average from the two k-grids was employed. A supercell of dimensions (10,10,10) Å and one k-point was used for calculations on the F_2 molecule.

The chemical shifts reported here are referenced to tetramethylsilane (TMS) by using benzene as a reference compound for the computational data and adding to the result the experimental chemical shift of benzene with respect to TMS.[22] In this way, results may be more easily compared between those obtained for finite SWNTs[23] and other molecular systems and infinite periodic pristine SWNTS.[22]

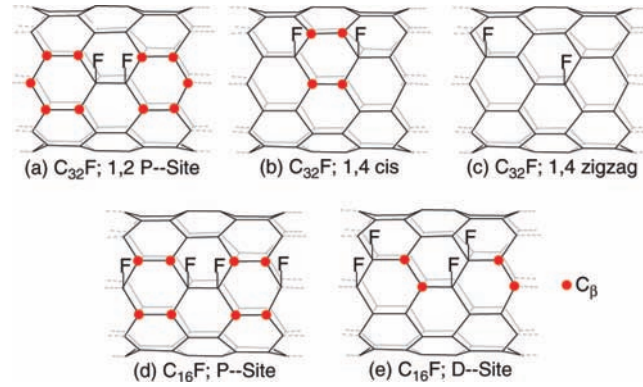

Figure 1. Illustrations of the (8,0) F-SWNTs with high C:F ratios studied in this work. In parts a−c the supercell contained two unit cells of the pristine tube (64 C atoms), and in parts d and e they consisted of a single unit cell (32 C atoms). The dashed lines denote a periodic system. For the P-sites and D-sites the fluorines were added to the pair of carbons making up a C−C bond parallel or diagonal to the tube axis, respectively. The C_β, whose distinctly high chemical shifts are singled out in Figure 6, are indicated by the red dots.

TABLE 1: The Monkhorst−Pack Grid of Dimension (1,1,m)[a] Used for the NMR Shielding Tensor Calculations on Fluorinated SWNTs and the Calculated Binding Energies of Fluorination, ΔE_{F_2}[b] (in kcal/mol)

$(n, 0)$	no. of C atoms	C:F	mode of addition[c]	m	ΔE_{F_2}
(8,0)	64	32:1	1,2 P-site	17	−89.25
(8,0)	64	32:1	1,4 cis	32	−75.64
(8,0)	64	32:1	1,4 zigzag	20[d]	−72.16
(8,0)	32	16:1	P-site	29	−75.70
(8,0)	32	16:1	D-site	29	−72.68
(8,0)	32	4:1	P-site	21	−71.54
(8,0)	32	2:1	P-site	21	−51.47
(9,0)	36	18:1	P-site	39/40	−73.54
(10,0)	40	20:1	P-site	16	−68.85

[a] If two values are given, the reported chemical shifts were calculated from an average obtained from both (1,1,m) k-grids. [b] $\Delta E_{F_2} = (E_{\text{F-SWNT}} - E_{\text{pristine}} - r\,E_{F_2})/r$, where r is the number of F_2 molecules added to the pristine tube. [c] The addition modes are illustrated in Figures 1 and 2. [d] Due to the very small band gap it was not possible to obtain reasonable convergence of the shieldings. The m given was used to optimize the geometry and to calculate the band gap.

Armchair tubes were not considered in this work since (at least pristine) infinite armchair SWNTs have a vanishing band gap. The computational NMR methodology presently available to us is not yet capable of treating zero-bandgap systems. Thus, like in previous NMR studies the computations were performed on selected finite-gap zigzag SWNTs.

To make a clear connection with our previous work on C−NR functionalized SWNTs with low to medium degrees of functionalization, we have included a number of model systems with high C:F ratios. The simplest systems chosen are direct analogues of the covalently functionalized C−NR SWNTs, where F_2 is added to a C−C bond either parallel (P) or diagonal (D) to the SWNT axis. Due to the rather formidable computational requirements of the NMR calculations, the configurational space for the F-SWNTs had to be restricted to a selected range, i.e., for a given C:F ratio not all possible isomers could be considered. The systems chosen here allow us to study a number of trends, such as adding more P-site functionalized C−C bonds per unit cell, and so on. Our initial calculations focused on

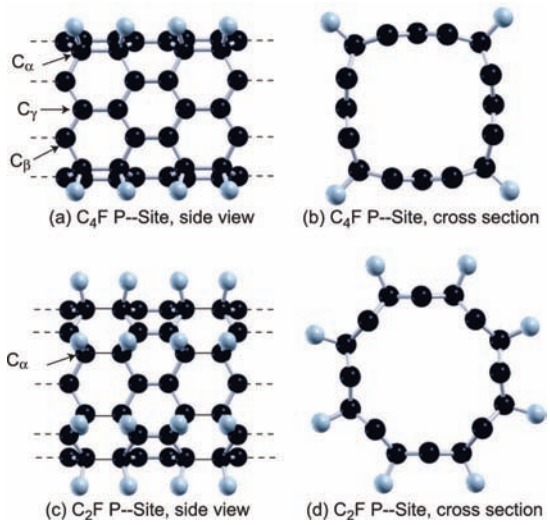

Figure 2. Side views and cross sections of the geometries of the (8,0) F-SWNTs considered in this work with (a, b) C_4F and (c, d) C_2F stoichiometries. A single unit cell containing 32 C atoms was used in both calculations. However, for clarity in the side views a double unit cell is shown. The dashed lines denote a periodic system.

fluorinated (8,0) SWNTs. For one type of fluorination pattern, we have also studied the (9,0) and (10,0) systems. Our results showed that the shifts of the functionalized carbons did not depend significantly on the radius of the tube considered. Since the results indicated that the NMR signals that are of highest interest, namely those of the carbons covalently bound to F, hardly depend on details of the SWNT structure, we believe that the selected set of systems is representative of the range of small to medium diameter semiconducting SWNTs.

For the carbons, we have chosen the following labeling: C_α is a fluorinated carbon and C_β is one of the carbons in a F-SWNT that has a particularly high chemical shift, as indicated in Figure 1. These are often, though not always, carbons separated by one C−C bond from a C_α. For the C_4F system, carbons separated from C_α by two C−C bonds are labeled as C_γ as in Figure 2.

III. Results and Discussion

A. Geometrical Parameters, Bonding Energies, and Band Gaps. STM experiments have shown that the side walls of F-SWNTs are covered with fluorine in a banded structure.[16] However, despite numerous theoretical studies[16,33,40−45] a consensus about the most favorable mode of bonding, as well as the electronic structure of the fluorinated tubes, has not yet been reached. For F-SWNTs with C_2F stoichiometry, geometries where the fluorines are added to the carbons perpendicular, or parallel to the tube axis have been proposed.[16] For the (10,10) SWNT, the perpendicular isomer was found to be slightly more stable.[16] On the contrary, DFT calculations on the same system indicated that the parallel geometry is favored.[42] DFTB has predicted fluorinated armchair and zigzag tubes to have a "ladder type" and "helical type" structure, respectively.[43] Calculations have yielded a wide range of electronic structures, varying from insulating to semiconducting to metallic.[41−43] We note that even though the terms 1,2- and 1,4-addition have been used to classify tubes with a low C:F ratio,[16] at a certain level of functionalization this nomenclature becomes ambiguous and depends upon how one chooses to number the carbon atoms.

The structures of the (8,0) F-SWNTs we have considered are illustrated in Figures 1 and 2. We note that the $C_{16}F$ species in parts d and e of Figure 1 could in principle be the products of either 1,2- or 1,4-addition, so this notation cannot be used unambiguously. Instead, we use the terms "P-site" and "D-site" to signify that the fluorines have been added to a bond *parallel* and *diagonal* to the tube axis, respectively. The fluorinated (9,0) and (10,0) systems which were studied consisted of a single unit cell of the pristine tube and two fluorines added to the carbons comprising the bond parallel to the tube axis, as illustrated for the (8,0) F-SWNT in Figure 1d.

It was not the purpose of this work to perform a systematic study of the energetics of the addition of fluorine to various SWNTs. Hence, we have not collected enough data to make definitive conclusions. However, examination of Table 1 hints at a number of trends. First of all, for a given mode (pattern) and degree of functionalization, fluorination appears to be more exothermic for narrower tubes. We see this to be the case for the (8,0)−(10,0) SWNTs which have one F_2 per unit cell attached to the P-site. This finding is in agreement with the results of ref 45, as well as those for zigzag tubes derivatized with N−H.[20]

For the (8,0) system at least, the 1,2-addition of fluorine to the carbons in the bond parallel to the tube axis gives the most negative ΔE_{F_2}. Fluorinating the bond diagonal to the tube axis as in Figure 1e is slightly less exothermic than the P-site, Figure 1d. This is in contrast to the NH-SWNTs, where functionalization at the D-site was found to be energetically more favorable.[20] For smaller diameter tubes the bond between the carbons in the D-site broke upon addition of NH, and the functionalized carbons were formally sp^2 hybridized. This bond does not break upon fluorination, yielding formally sp^3 hybridized carbons.

The magnitude of ΔE_{F_2} decreases with decreasing C:F ratio. That is, adding more and more fluorines to the tubes becomes progressively less exothermic. As the stoichiometry of the (8,0) F-SWNT is varied from $C_{32}F$ to C_4F, the magnitude of ΔE_{F_2} decreases by ∼20 kcal/mol. A further doubling of the degree of functionalization to saturation results in a similar decrease in the binding energy per F_2 unit.

As Figures 3−5 show, the band gaps of the F-SWNTs are strongly dependent upon the degree of functionalization, the sites which have been fluorinated, and the radius of the tube. For example, the band gaps of the (8,0) tubes with a stoichiometry of $C_{32}F$ vary from 0.02 to 0.40 eV. The saturated C_2F tube, on the other hand, has a gap of 1.00 eV. In general, it appears that for low degrees of fluorination the gaps of the F-SWNTs are smaller than those of the pristine tubes, whereas for high degrees of fluorination the opposite is true.

For low degrees of fluorination (Figures 3 and 5) the functional groups give rise to new bands and break the degeneracy of others, compared to the pristine species. In particular, a new band is introduced just above the Fermi level. In all cases, this conduction band becomes nearly dispersionless about halfway between Γ and Z. For the (8,0) 1,4 zigzag F-SWNT illustrated in Figure 1c this whole band is nearly flat. However, the band structure of the pristine SWNTs is still very clearly reflected in the band structures of these high C:F ratio F-SWNTs. On the other hand, the band structures of the F-SWNTs with stoichiometries of C_4F and C_2F (Figure 4) are substantially different from those of the pristine (8,0) system. In particular, the band gap of the saturated F-SWNT is no longer at the Γ point, but at X instead. The high degree of fluorination introduces many nearly dispersionless bands. These results

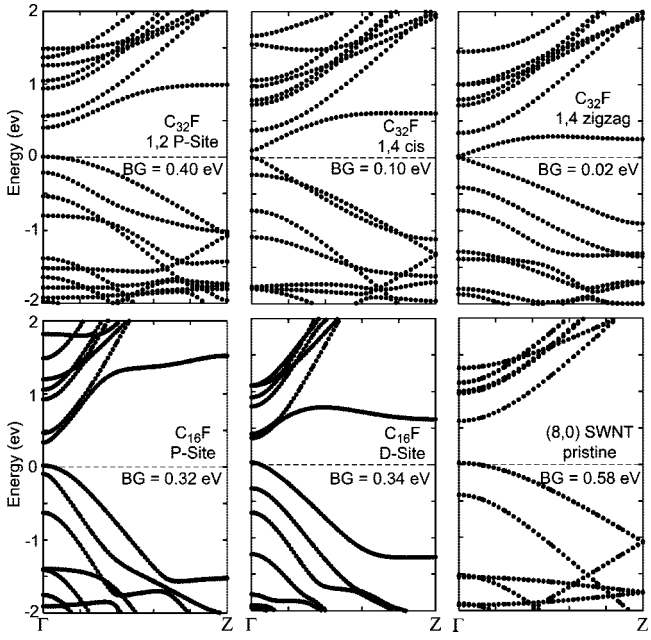

Figure 3. Band structures and band gaps (BG) of the (8,0) F-SWNTs illustrated in Figure 1. The Fermi level has been set to zero. For comparison, the band structure of the pristine (8,0) SWNT is also shown.

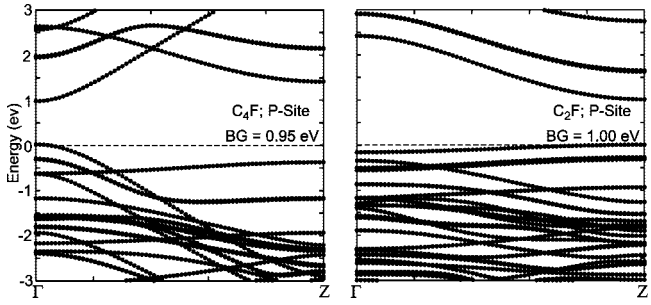

Figure 4. Band structures and band gaps (BG) of the (8,0) F-SWNTs illustrated in Figure 2. The Fermi level has been set to zero.

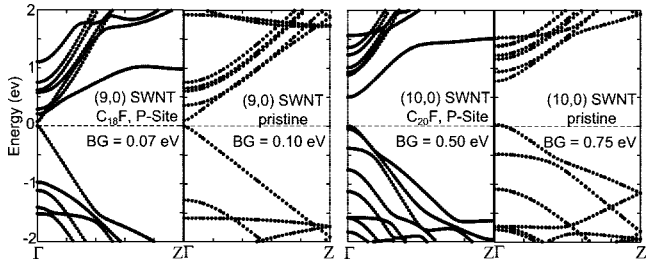

Figure 5. Band structures and band gaps (BG) of the (9,0) and (10,0) F-SWNTs functionalized at the P-site as in Figure 1d. The Fermi level has been set to zero. For comparison, the band structures of the pristine SWNTs are also shown.

indicate that different degrees and modes (patterns) of fluorination can give rise to F-SWNTs with a multitude of electronic structures.

B. ^{13}C NMR Chemical Shifts of Fluorinated SWNTs. We have calculated the ^{13}C NMR chemical shifts of the F-SWNTs described above in Section 3A. One of the aims was to see how well the shifts of the fluorinated carbons compare with experimental data, and also with previous calculations performed on a $C_{80}H_{20}$ finite (5,5) fragment.[27] Moreover, we wanted to investigate if NMR could be used to determine the degree of functionalization of F-SWNTs, and the sites to which the fluorines bind.

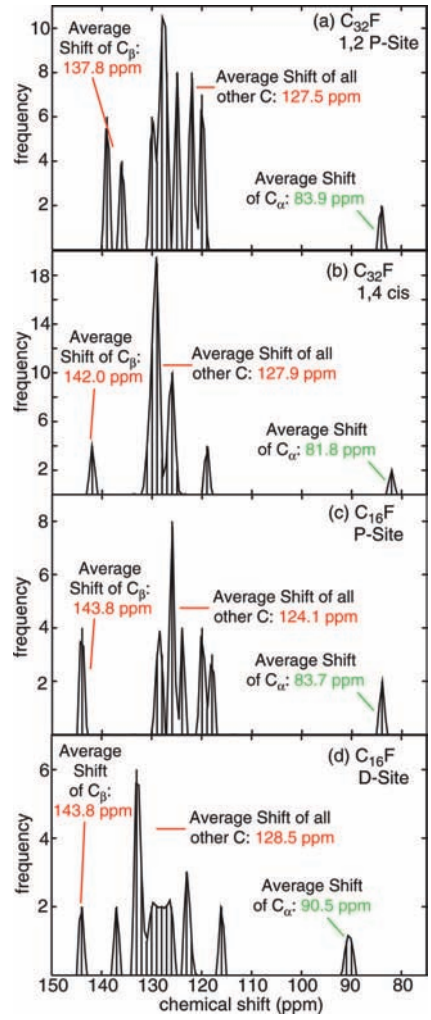

Figure 6. Calculated histograms of the ^{13}C NMR chemical shifts of an (8,0) SWNT with different degrees and modes of functionalization. The tubes considered have a high C:F ratio and are illustrated in Figure 1, where the C_β carbons are also pointed out. The shift of the carbons in a pristine (8,0) SWNT is 131.7 ppm.

First, let us consider the shifts of the (8,0) F-SWNTs illustrated in Figure 1. All of these have high C:F ratios since the supercell contained either one or two unit cells of the pristine tube, and only two fluorine atoms. The 1,4 zigzag F-SWNT shown in Figure 1c has a very small band gap of 0.02 eV. Unfortunately, the small band gap prevented us from converging the shieldings sufficiently with respect to the *k*-grid used.

Figure 6 displays the calculated ^{13}C NMR shift histograms for the four F-SWNTs we could study. The shifts of the fluorinated sp^3 carbons (C_α) range from 81.8 to 90.5 ppm. With the exception of the tube functionalized at the D-site, they are in excellent agreement with the experimentally observed signal of $\delta = 83.5$ ppm attributed to the C_α.[27] Our results suggest that NMR cannot be used to discriminate between 1,2- and 1,4-addition, since the shifts for the C_α in the 1,2 P-site and 1,4 cis F-SWNTs differ by only 2.1 ppm. In contrast, the calculations in ref 27 concluded that a shift of ~80 ppm was indicative of 1,2-addition. However, the computations were performed on a finite armchair tube whose dangling bonds were saturated with hydrogen. Our previous work has shown that finite length and capping may affect the calculated chemical shifts of pristine SWNTs significantly.[23,22] The effect of doubling the degree of P-site functionalization has virtually no effect on the shifts of the C_α (compare parts a and c of Figure 6, which are both fluorinated at the P-site).

To relate this work to previous calculations, we have previously found that for NH derivatized zigzag tubes with $n \leq 15$, functionalization at the D-site led to the breaking of the C−C bond.[21,20] This is because this bond is strained in narrow tubes due to the high degree of curvature. The functionalized carbons were therefore formally either sp^2 or sp^3 hybridized, depending upon whether the derivatized C−C bond broke or not. The shifts of the D-site carbons were dependent upon the hybridization of the functionalized carbon atoms, and varied between 60 and 140 ppm. On the other hand, the C−C bonds of tubes where NH was added to the P-site did not break, i.e., the carbon atoms were formally sp^3 hybridized. For this mode of functionalization, the shifts of the derivatized carbons were all calculated to be ∼45 ppm. We therefore proposed that the shifts of the derivatized carbons could be used to determine which bond has been functionalized,[21] and in case of D-site functionalization, the radius of the SWNT.[20]

For the fluorinated tubes we see a very different behavior. Addition of fluorine elongates the C−C bonds, but they do not break. Thus, for all of the F-SWNTs we have considered, the C_α are formally sp^3 hybridized. In the pristine (8,0) SWNT the lengths of the bonds parallel and diagonal to the tube axis are 1.42 and 1.44 Å, respectively. Upon fluorination they elongate by an amount less than 0.2 Å. For example, the $C_\alpha-C_\alpha$ bonds were calculated as being 1.56 to 1.58 and 1.60 Å for the two P-site type and the one D-site F-SWNT considered, respectively. The $C_\beta-C_\alpha$ bonds ranged from 1.50 to 1.53 Å in all of the systems we studied. The mode and degree of functionalization does not drastically affect the local environment around the $C_\alpha-F$ units. We therefore propose that this is the reason why the shifts of the C_α carbons are nearly the same for all of the F-SWNTs we considered. The somewhat larger $C_\alpha-C_\alpha$ bond elongation of the high C:F D-site system is most likely the reason for the slightly higher chemical shifts of the C_α, i.e., this species exhibits the onset of a behavior akin to the D-site NH functionalized systems mentioned in the previous paragraph. However, since the $C_\alpha-C_\alpha$ bond does not break for the narrow (8,0) tube, the shift of the C_α is not drastically different than in the other systems considered. For tubes with larger diameters, the $C_\alpha-C_\alpha$ bonds for the D- and P-site functionalizations should become more similar, along with their chemical shifts.

What about the shifts of the other carbons in the tube, that is those which have not reacted with fluorine? How do they compare with that of a pristine (8,0) SWNT, for which $\delta = 131.7$ ppm? Examination of Figure 6 first of all shows a significant broadening of the signals originating from these carbons. In all cases there are a few (more or less) isolated peaks found at $\delta \geq$ ca. 138 ppm.

For the 1,2 P-site the shifts with an average at 137.8 ppm are due to the 10 carbons comprising two hexagons which contain a C_α. These carbons are labeled with red dots in Figure 1a (C_β). The average shift of the rest of the unfluorinated carbons, 127.5 ppm, is slightly lower than that in the pristine tube. For comparison, we also performed computations using the optimized geometries of the fluorinated systems, but with the F atoms taken off. An analysis of the data showed that much of the NMR peak broadening of the sidewall carbons can be attributed to the geometrical distortion of the nanotube. This finding is similar to those for NH-functionalized systems.[21] Electronic effects from the presence of the fluorines are most pronounced for the C_β carbons (red dots in Figure 1), apart from the C_α themselves for which the chemical shift changed from 83.9 to well over 200 ppm, upon removal of the fluorines. The fact that the other carbons are little affected electronically by the presence of the fluorine atoms shows that the C−F perturbation is very localized. We have found similar trends for the other systems investigated here and will discuss some, but not all, of them explicitly.

For the 1,4 cis species, the shifts with $\delta = 142$ ppm arise from the four C_β carbons which bind to the C_α along a diagonal bond, see Figure 1b. There are two other carbons which also bind to C_α via a parallel bond. Their shifts, however, are not too different than those of a pristine tube and are found at $\delta = 130.4$ ppm. We have taken the average of the shifts not including the C_α and the four highest ones (C_β, since their signals are relatively well isolated from the bulk of the spectrum). This average of 127.9 ppm is slightly less than that of a pristine (8,0) SWNT.

For the P-site with $C_{16}F$ stoichiometry, the average of the shifts of the four carbons directly attached to the C_α is found at 143.8 ppm. When the fluorines are removed from the tube, the signal from these carbons increases somewhat to $\delta = 159.4$ ppm. This indicates that both geometrical distortions of the tube due to fluorination and electronic effects bring about the high shift of the C_β. The average shift of the rest of the carbons, 124.1 ppm, is somewhat lower than that for the pristine system.

For the D-site, the carbons with the two highest shifts at 143.8 ppm bind to the C_α in a bond parallel to the tube axis. The two other high shifts at ∼137 ppm originate from carbons which are not at all bound to the C_α, in fact they are almost directly on the opposite side of the tube. We include them in the average chemical shift of the bulk of the sample, 128.5 ppm, which is somewhat lower than that for the pristine tube. We note that the peak arising from the carbons which we include in this average is significantly broader than that for the other systems we have considered. This could be because functionalization of the D-site yields F-SWNTs with fewer symmetry elements than the other systems we have considered. For comparison, previously we found that the spectra of SWNTs with Stone−Wales defects were also considerably more complicated when the defect was generated by a 90 °C rotation of a C−C bond diagonal to the tube axis, as compared to a rotation around the parallel bond.[24]

Our results so far indicate that the local environment around the fluorinated carbons is insensitive to the pattern and degree of functionalization. As a result, the shifts of the C_α are insensitive to these parameters, for low degrees of functionalization. To see if this is also the case for high degrees of functionalization, we have considered the (8,0) F-SWNTs with C_4F and C_2F stoichiometries, illustrated in Figure 2. The histograms in Figure 7 indicate that once again the signal arising from the fluorinated carbons is found at $\delta \sim 83.5$ ppm. We note that in an isolated F-SWNT, the tubes with C_4F and C_2F would afford 3 and 2 symmetry inequivalent carbons, respectively. The hexagonal unit cell used for the computations has broken this symmetry slightly, and for example, we see two peaks arising from the C_α in Figure 7a. The symmetry breaking might indicate interactions between separated nanotubes in the periodic lattice and slight dissymmetries due to finite convergence criteria in the geometry optimizations. However, in all cases the splitting of the shifts is less than 2 ppm, indicating that the periodic images do not have a strong effect on each other.

Apart from the C_α carbons, the C_4F tube has two other symmetry inequivalent carbons, labeled as C_β and C_γ in Figure 2a. The former are directly bound to the C_α carbons and have a shift of 143.5 ppm. This value is quite similar to the high shifts attributed to the carbons labeled in red in Figure 1, for

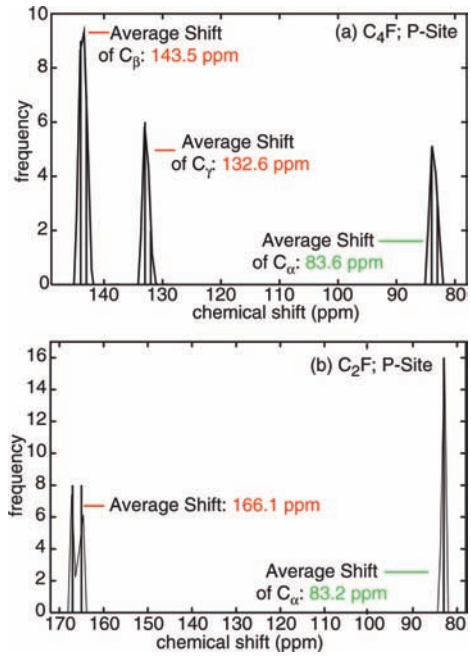

Figure 7. Calculated histograms of the ^{13}C NMR chemical shifts of an (8,0) SWNT with different degrees of functionalization. The tubes considered have a low C:F ratio and are illustrated in Figure 2. The shift of the carbons in a pristine (8,0) SWNT is 131.7 ppm.

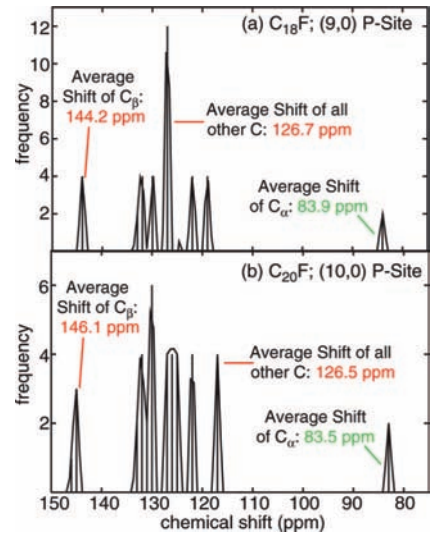

Figure 8. Calculated histograms of the ^{13}C NMR chemical shifts of a (9,0) and (10,0) SWNT fluorinated at the P-site, as illustrated for the (8,0) SWNT in Figure 1d. The shifts of the carbons in a pristine (9,0) and (10,0) SWNT are 122.2 and 127.9 ppm, respectively.

the tubes with low degrees of functionalization. The C_γ carbons afford a shift that is not too different from that of a pristine (8,0) tube.

The saturated C_2F tube has one set of carbons whose shift is substantially higher than those calculated for any other system, at 166.1 ppm. In this geometry, but without the fluorines, these carbons would afford a shift of 159.8 ppm, indicating once more that geometrical distortion is primarily responsible for their high shifts. It is significant that at high degrees of functionalization, the shifts of sets of symmetry equivalent unfunctionalized carbons become well isolated from those of others. This suggests that perhaps these shifts may be used to determine where the fluorines bind to the nanotube surface, i.e., the molecular structure of the F-SWNTs and the bonding pattern.

It is interesting to note that the ^{13}C NMR chemical shifts of the C_α in a T_h-symmetric $C_{60}F_{24}$ functionalized fullerene were also measured to be 83.5 ppm.[46] Since this signal is the same for both F-SWNTs and a fluorinated fullerene, it suggests that the shifts of the C_α do not depend upon the curvature of the carbon framework. To study this further, we have considered a (9,0) and (10,0) SWNT fluorinated at the P-site, as illustrated for the (8,0) system in Figure 1d. Comparison of the histograms in Figures 8 and 6c indicates that this is indeed the case: for the P-site the shift varied by less than 0.5 ppm for the three different diameters studied. We therefore conclude that the shifts of the C_α in tubes narrower and wider than those we have studied should be very similar to those in the (8,0) systems. The other features of the NMR shift histograms in the (9,0) and (10,0) F-SWNTs are also very similar to that of the (8,0). That is, there are peaks at $\delta > 140$ ppm, which correspond to the carbons denoted in red in Figure 1d. The average shifts of the other unfunctionalized carbons are somewhat higher than those in the pristine tube for the (9,0) and lower than in the (10,0). However, they do not differ dramatically from those in the pristine tubes.

The T_h -$C_{60}F_{24}$ system affords a carbon in an environment where it has a double bond to one carbon and a single bond to each of two fluorinated C_α. That is, the local geometry around this carbon is similar to that illustrated in Figure 2c,d for the (8,0) system. The difference is, of course, that the fullerene also contains pentagonal rings. The NMR chemical shift of this carbon, at $\delta = 145.9$ ppm,[46] is 20 ppm lower than that of the unfluorinated carbons in the tube with C_2F stoichiometry. However, it is quite similar to the signals arising from the C_β indicated in Figures 1 and 2a.

Besides the isotropic shifts, which represent the average of the shielding tensor principal components, the nuclear magnetic shielding anisotropy ($\Delta\sigma$) is another important NMR parameter. Differences in the isotropic shifts of the carbons in the fluorinated systems may be caused by a combination of changes in the individual shielding tensor components. Therefore, we also report shielding tensor data in this work. Instead of reporting $\Delta\sigma$ for each of the SWNTs, we decided to provide a graphical representation of the shielding tensors for a representative system. Figure 9 shows the shielding tensors for the three distinct carbon sites C_α, C_β, and C_γ of a fluorinated (8,0) SWNT with a C:F ratio of 4:1 (the C_4F system of Figure 2). For the unfunctionalized carbons, the shielding tensors calculated for this fluorinated SWNT are strongly anisotropic. This is similar to our previous findings for pristine and covalently functionalized SWNTs, as well as those with Stone−Wales defects.[22−24] The tensor for a pristine (8,0) tube (see ref 24) affords a large positive principal component perpendicular to the SWNT sidewall (the radial component), and small negative components tangential to the sidewall (ortho-radial and -axial components; the axial component is in the direction of the SWNT axis). The shielding tensor for C_γ is quite similar to the one in the pristine SWNT both in shape/orientation and in magnitude. Thus, as seen in Figure 7a, the isotropic C_γ shift is similar to that of the pristine system. The tensor for C_β has a similar shape, too, but with more pronounced negative axial and ortho-radial components and a reduced radial component, leading to the higher chemical shift (Figure 7). The shielding tensor for C_α is very different, as one might have expected from its low isotropic chemical shift. The tensor is much less anisotropic (a perfectly isotropic positive tensor would be represented by a blue sphere in Figure 9),

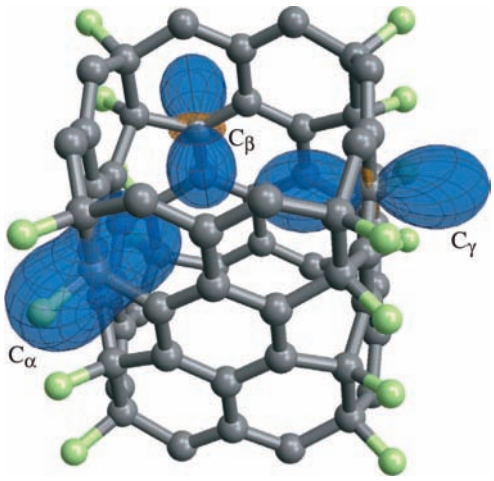

Figure 9. Shielding tensors for the three distinct carbon sites C_α, C_β, and C_γ of a (8,0) fluorinated SWNT with C_4F stoichiometry (Figure 2). The tensors are represented as polar plots; see refs 24 and 47 for details. The plots indicate the tensor orientation as well as the relative magnitudes and signs of the principal components (blue/orange = positive/negative).

with the three components of the same sign reinforcing each other to produce a significantly more shielded C_α nucleus. The largest component is still in the radial direction, however, which is similar to the shielding tensors of the other carbons in this fluorinated SWNT.

IV. Conclusions

The results of first-principles computations of chemical shifts on infinite periodic semiconducting fluorinated SWNTS have validated the assignment of the chemical shift of fluorinated carbons, C_α, in these systems to be around 83.5 ppm. No significant changes of this shift were noted in a range of different systems with different functionalization patterns and degrees of fluorination. This shift is also insensitive to the SWNT diameter. The computed results agree very well with experimental data from ref 27. This NMR signal is therefore an excellent indicator of the degree of functionalization for a heterogeneous fluorinated SWNT sample.

For low degrees of fluorination, a number of carbons, labeled as C_β, were found to have chemical shifts substantially higher than the bulk of the sidewall carbons. Considering the computations of the (8,0) systems with C:F ratios close to saturation, the chemical shifts of the C_β, C_γ (see Figure 7) become rather easy to interpret. Therefore, at a high degree of functionalization the shifts of carbons neighboring C_α might be very useful experimental indicators of the functionalization pattern.

Acknowledgment. We thank Thao Vo and Catherine Johnson for assistance with a subset of the computations which were performed as part of their undergraduate research projects at SUNY Buffalo. J.A. acknowledges support from the Center of Computational Research at SUNY Buffalo and is grateful for financial support of his research from the CAREER program of the National Science Foundation (grant no. CHE-0447321).

References and Notes

(1) Close, G. F.; Yasuda, S.; Paul, B.; Fujita, S.; Wong, H. S. P. *Nano Lett.* **2008**, *8*, 706–709.

(2) Itkis, M. E.; Yu, A.; Haddon, R. C. *Nano Lett.* **2008**, *8*, 2224–2228.

(3) Snow, E. S.; Perkins, F. K.; Houser, E. J.; Badescu, S. C.; Reinecke, T. L. *Science* **2005**, *307*, 1942–1945.

(4) Tang, X.; Bansaruntip, S.; Nakayama, N.; Yenilmez, E.; Chang, Y.-I.; Wang, Q. *Nano Lett.* **2006**, *6*, 1632–1636.

(5) Tasis, D.; Tagmatarchis, N.; Bianco, A.; Prato, M. *Chem. Rev.* **2006**, *106*, 1105–1136.

(6) Wu, Y.; Phillips, J. A.; Liu, H.; Yang, R.; Tan, W. *ACS Nano* **2008**, *2*, 2023–2028.

(7) Mickelson, E. T.; Huffman, C. B.; Rinzler, A. G.; Smalley, R. E.; Hauge, R. H.; Margrave, J. L. *Chem. Phys. Lett.* **1998**, *296*, 188–194.

(8) Khabashesku, V. N.; Billups, W. E.; Margrave, J. L. *Acc. Chem. Res.* **2002**, *35*, 1087–1095.

(9) Saini, R. K.; Chiang, I. W.; Peng, H.; Smalley, R. E.; Billups, W. E.; Hauge, R. H.; Margrave, J. L. *J. Am. Chem. Soc.* **2003**, *125*, 3617–3621.

(10) Pulikkathara, M. X.; Kuznetsov, O. V.; Khabashesku, V. N. *Chem. Mater.* **2008**, *20*, 2685–2695.

(11) Stevens, J. L.; Huang, A. Y.; Peng, H.; Chiang, I. W.; Khabashesku, V. N.; Margrave, J. L. *Nano Lett.* **2003**, *3*, 331–336.

(12) Zhang, L.; Kiny, V. U.; Peng, H.; Zhu, J.; Lobo, R. F. M.; Margrave, J. L.; Khabashesku, V. N. *Chem. Mater.* **2004**, *16*, 2055–2061.

(13) Dillon, E. P.; Crouse, C. A.; Barron, A. R. *ACS Nano* **2008**, *2*, 156–164.

(14) Gu, Z.; Peng, H.; Hauge, R. H.; Smalley, R. E.; Margrave, J. L. *Nano Lett.* **2002**, *2*, 1009–1013.

(15) Bettinger, H. F.; Peng, H. *J. Phys. Chem. B* **2005**, *109*, 23218–23224.

(16) Kelly, K. F.; Chiang, I. W.; Mickelson, E. T.; Hauge, R. H.; Margrave, J. L.; Wang, X.; Scuseria, G. E.; Radloff, C.; Halas, N. J. *Chem. Phys. Lett.* **1999**, *313*, 445–450.

(17) Zhang, L.; Zhang, J.; Schmandt, N.; Cratty, J.; Khabashesku, V. N.; Kelly, K. F.; Barron, A. R. *Chem. Commun.* **2005**, 5429–5431.

(18) Zurek, E.; Autschbach, J. Ab-Initio NMR Computations for Carbon Nanotubes. In *Encyclopedia of Nanoscience and Nanotechnology*, 2nd ed.; Nalwa, H. S., Ed.; American Scientific Publishers: Stevenson Ranch, CA, in press.

(19) Zurek, E.; Autschbach, J. Density Functional Studies of the 13 C NMR Chemical Shifts in Single-Walled Carbon Nanotubes. In *Computation in Modern Science and Engineering, Proceedings of the International Conference on Computational Methods in Science and Engineering 2007*; Simos, T. E., Maroulis, G., Eds.; American Institute of Physics: College Park, MD, 2007; Vol. 2, part B, pp 1425−1428.

(20) Zurek, E.; Pickard, C. J.; Autschbach, J. *J. Phys. Chem. C* **2008**, *112*, 9267–9271.

(21) Zurek, E.; Pickard, C. J.; Autschbach, J. *J. Am. Chem. Soc.* **2007**, *129*, 4330–4339.

(22) Zurek, E.; Pickard, C. J.; Walczak, B.; Autschbach, J. *J. Phys. Chem. A* **2006**, *110*, 11995–12004.

(23) Zurek, E.; Autschbach, J. *J. Am. Chem. Soc.* **2004**, *126*, 13079–13088.

(24) Zurek, E.; Pickard, C. J.; Autschbach, J. *J. Phys. Chem. C* **2008**, *112*, 11744–11750.

(25) Lai, L.; Lu, J.; Song, W.; Ni, M.; Wang, L.; Luo, G.; Zhou, J.; Mei, W. N.; Gao, Z.; Yu, D. *J. Phys. Chem. C* **2008**, *112*, 16417–16421.

(26) Zeng, L.; Alemany, L. B.; Edwards, C. L.; Barron, A. R. *Nano Res.* **2008**, *1*, 72–88.

(27) Alemany, L. B.; Zhang, L.; Zheng, L.; Edwards, C. L.; Barron, A. R. *Chem. Mater.* **2007**, *19*, 735–744.

(28) Cahill, L. S.; Yao, Z.; Adronov, A.; Penner, J.; Moonoosawmy, K. R.; Kruse, P.; Goward, G. R. *J. Phys. Chem. B* **2004**, *108*, 11412–11418.

(29) Zhao, J.; Balbuena, P. B. *J. Phys. Chem. C* **2008**, *112*, 3482–3488.

(30) Zhao, J.; Balbuena, P. B. *J. Phys. Chem. C* **2008**, *112*, 13175–13180.

(31) Besley, N. A.; Noble, A. *J. Chem. Phys.* **2008**, *128*, 101102–4.

(32) Sebastiani, D.; Kudin, K. N. *ACS Nano* **2008**, *2*, 661–668.

(33) Bettinger, H. F. *Org. Lett.* **2004**, *6*, 731–734.

(34) Segall, M. D.; Lindan, P. J. D.; Probert, M. J.; Pickard, C. J.; Hasnip, P. J.; Clark, S. J.; Payne, M. C. *J. Phys.: Condens. Matter* **2002**, *14*, 2717–2744.

(35) Clark, S. J.; Segall, M. D.; Pickard, C. J.; Hasnip, P. J.; Probert, M. J.; Refson, K.; Payne, M. C. *Z. Kristallogr.* **2005**, *220*, 567–570.

(36) Perdew, J. P.; Burke, K.; Wang, Y. *Phys. Rev. B* **1996**, *54*, 16533–16539.

(37) Vanderbilt, D. *Phys. Rev. B* **1990**, *41*, 7892–7895.

(38) Pickard, C. J.; Mauri, F. *Phys. Rev. B* **2001**, *63*, 245101–13.

(39) Yates, J. R.; Pickard, C. J.; Mauri, F. *Phys. Rev. B* **2007**, *76*, 024401–11.

(40) Van Lier, G.; Ewels, C. P.; Zuliani, F.; De Vita, A.; Charlier, J. C. *J. Phys. Chem. B* **2005**, *109*, 6153–6158.
(41) Seifert, G.; Köhler, T.; Frauenheim, T. *Appl. Phys. Lett.* **2000**, *77*, 1313–1315.
(42) Kudin, K. N.; Bettinger, H. F.; Scuseria, G. E. *Phys. Rev. B* **2001**, *63*, 045413.
(43) Park, K. A.; Choi, Y. S.; Lee, Y. H.; Kim, C. *Phys. Rev. B* **2003**, *68*, 045429.
(44) Bauschlicher, C. W., Jr. *Chem. Phys. Lett.* **2000**, *322*, 237–241.
(45) Bettinger, H. F.; Kudin, K. N.; Scuseria, G. E. *J. Am. Chem. Soc.* **2001**, *123*, 12849–12856.
(46) Denisenko, N. I.; Troyanov, S. I.; Popov, A. A.; Kuvychko, I. V.; Zemva, B.; Kemnitz, E.; Strauss, S. H.; Boltalina, O. V. *J. Am. Chem. Soc.* **2004**, *126*, 1618–1619.
(47) Hansen, A. E.; Bouman, T. *J. Chem. Phys.* **1989**, *91*, 3552–3560.

JP810523X